PROCEEDINGS, TOUGH Symposium 2012
Lawrence Berkeley National Laboratory, Berkeley, California, September 17-19, 2012

DEVELOPMENT OF AN ADVANCED THERMAL-HYDROLOGICAL-MECHANICAL MODEL FOR CO_2 STORAGE IN POROUS AND FRACTURED SALINE AQUIFERS

by P. H. Winterfeld[*], Y.-S. Wu[*], K. Pruess[†], and C. Oldenburg[†]

[*]Colorado School of Mines
Department of Petroleum Engineering
1613 Illinois St., Golden, CO 80401
pwinterf@mines.edu

[†]Lawrence Berkeley National Laboratory
1 Cyclotron Road
Berkeley CA 94720

ABSTRACT

We developed a fully coupled simulator for modeling thermal-hydrologic-mechanical (THM) effects in fractured and porous media saline aquifers. The multiphase and heat flow formulation is that for TOUGH2-MP, the starting point for our simulator. The geomechanical equations relating stresses and displacements are combined to yield an equation for mean stress as a function of pressure and temperature that is added to the formulation. In addition, theories of poroelasticity and experimental studies have correlated porosity and permeability to effective stress, and we incorporate those dependencies into our simulator as well.

We also developed an advanced physical property module, ECO2M, designed for CO_2 sequestration in saline aquifers. It includes the relevant properties of H_2O–NaCl–CO_2 mixtures for the temperature, pressure, and salinity conditions of interest. Three fluid phases may be present: (1) an aqueous phase that could contain some dissolved CO_2, (2) a liquid CO_2-rich phase that could contain dissolved water, and (3) a gaseous CO_2-rich phase that could also contain dissolved water. Salt may be present in the aqueous phase or as a solid precipitate.

The simulator formulation and numerical implementation are verified using analytical solutions and an example problem from the literature.

MEAN STRESS EQUATION

Our simulator is a modification of TOUGH2-MP (Zhang et al., 2008), which solves mass and energy balances over the simulation domain using the integral finite difference method on an unstructured grid. We extend its formulation to a fully coupled THM one by adding a governing equation for mean stress to the mass and energy balances. The mean stress equation is derived in this section.

The stress-strain relationship for an elastic fluid-filled porous media under nonisothermal conditions is (McTigue, 1986)

$$\bar{\bar{\tau}} - \left(\alpha P + 3\beta K(T - T_{ref})\right)\bar{\bar{I}} = 2G\bar{\bar{\epsilon}} + \lambda(\mathrm{tr}\bar{\bar{\epsilon}})\bar{\bar{I}} \quad (1)$$

where T_{ref} is reference temperature, β is linear thermal expansion coefficient, K is bulk modulus, G is shear modulus, λ is the Lamé parameter, and α is the Biot coefficient. Two terms are subtracted from the normal stress tensor components in this thermo-poroelastic extension of Hooke's law. The first is the pressure term from poroelasticity theory, and the second is the temperature term from thermo-elasticity theory. We obtain the multi-porosity generalization of Equation 1 from Bai et al. (1993) while retaining the temperature term

$$\bar{\bar{\tau}} - \left(\sum \alpha_k P_k + 3\beta K(T_k - T_{ref})\right)\bar{\bar{I}} = 2G\bar{\bar{\epsilon}} + \lambda(\mathrm{tr}\bar{\bar{\epsilon}})\bar{\bar{I}} \quad (2)$$

where subscript k refers to the porous continuum (fracture or matrix for double-porosity systems). Expressions for the generalized Biot coefficients α_k for a double-porosity medium have been presented by Wilson and Aifantis (1982)

$$\alpha_1 = 1 - \frac{K}{K_*};\ \alpha_2 = \frac{K}{K_*}\left(1 - \frac{K_*}{K_s}\right) \quad (3)$$

where K_s is the solid modulus, K_* is the modulus of the porous medium without the fractures, subscript 1 refers to the fractures, and subscript 2 to the matrix.

We obtain a relationship between volumetric strain, ϵ_v, and mean stress, τ_m, by taking the trace of Equation 2:

$$K\epsilon_v = \tau_m - \sum \alpha_k P_k - 3\beta K(T_k - T_{ref}) \quad (4)$$

The strain tensor and the displacement vector $\bar{u}$ are related by

$$\bar{\bar{\epsilon}} = \frac{1}{2}(\nabla\bar{u} + \nabla\bar{u}^t) \quad (5)$$

and the static equilibrium equation is

$$\nabla \cdot \bar{\bar{\tau}} + \bar{F} = 0 \quad (6)$$

where $\bar{F}$ is the body force. We combine Equations 2, 5, and 6 to obtain the thermo-poroelastic Navier equations for a multi-porosity medium

$$\nabla(\sum \alpha_k P_k + 3\beta K T_k) + (\lambda + G)\nabla(\nabla \cdot \bar{u}) + G\nabla^2\bar{u} + \bar{F} = 0 \quad (7)$$

Taking the divergence of Equation 7, noting the divergence of the displacement vector is the volumetric strain, and combining with Equation 4 yields the governing equation for mean stress:

$$\frac{3(1-\nu)}{1+\nu}\nabla^2\tau_m + \nabla \cdot \bar{F} - \frac{2(1-2\nu)}{1+\nu}\nabla^2(\sum \alpha_k P_k + 3\beta K T_k) = 0 \quad (8)$$

where ν is Poisson's ratio.

ROCK PROPERTY CORRELATIONS

Correlations have been developed for porosity as a function of effective stress and permeability as a function of porosity. A theory of hydrostatic poroelasticity (Zimmerman et al., 1986) has been proposed that accounts for the coupling of rock deformation with fluid flow inside the porous rock. Porosity as a function of effective stress is derived from this theory

$$d\phi = -\left[\frac{1}{K}(1 - \phi) - C_r\right] d\tau' \quad (9)$$

where τ' is effective stress and C_r is rock grain compressibility.

Porosity is the ratio of fluid to bulk (solid plus fluid) volume. Bulk volume, V, is related to volumetric strain by

$$V = V_0(1 - \epsilon_v) = V_i \frac{(1-\epsilon_v)}{(1-\epsilon_{v,i})} \quad (10)$$

where V_0 is zero strain volume and subscript i refers to reference conditions.Gutierrez et al. (2001) presented expressions for solid volume change with pressure and effective stress, which when combined with the above yield the following expression for porosity

$$\phi = 1 - \frac{(1-\phi_i)V_i + \frac{(1-\phi_i)}{K_s}(P - P_i) - \frac{1}{K_s}(\tau' - \tau_i')}{V_i \frac{(1-\epsilon_v)}{(1-\epsilon_{v,i})}} \quad (11)$$

Rutqvist et al. (2002) presented the following function for porosity, obtained from laboratory experiments on sedimentary rock (Davies and Davies, 1999)

$$\phi = \phi_r + (\phi_0 - \phi_r)e^{-a\tau'} \quad (12)$$

where ϕ_0 is zero effective stress porosity, ϕ_r is high effective stress porosity, and the exponent "a" is a parameter. They also presented an associated function for permeability in terms of porosity:

$$k = k_0 e^{c\left(\frac{\phi}{\phi_0} - 1\right)} \quad (13)$$

Ostensen (1986) studied the relationship between effective stress and permeability for tight gas sands and approximated permeability as

$$k^n = D\ln\frac{\tau'^{,*}}{\tau'} \quad (14)$$

where exponent n is 0.5, "D" is a parameter, and $\tau'^{,*}$ is effective stress for zero permeability, obtained by extrapolating permeability versus effective stress on a semi-log plot.

Verma and Pruess (1988) presented a power law expression relating permeability to porosity

$$\frac{k-k_c}{k_0-k_c} = \left(\frac{\phi-\phi_c}{\phi_0-\phi_c}\right)^n \quad (15)$$

where k_c and ϕ_c are asymptotic values of permeability and porosity, respectively, and exponent n is a parameter.

The above correlations for porosity and permeability have been incorporated into our simulator.

ECO2M FLUID PROPERTY MODULE

We developed an advanced fluid property module called ECO2M (Pruess, 2011). ECO2M was designed for CO_2 sequestration in saline aquifers. It includes a description of the relevant properties of H_2O–NaCl–CO_2 mixtures that is highly accurate for the temperature, pressure, and salinity conditions of interest (between 10 and 110°C, pressure less than 600 bar, and salinity up to full halite saturation). Three fluid phases may be present: an aqueous phase that could contain some dissolved CO_2, a liquid CO_2-rich phase that could contain dissolved water, and a gaseous CO_2-rich phase that could also contain dissolved water. The partitioning of H_2O and CO_2 between the phases is modeled as a function of temperature, pressure, and salinity, using a slightly modified version of the correlations of Spycher and Pruess (2005).

The ECO2M fluid property correlations are identical to those of the earlier, less advanced ECO2N fluid property module (Pruess and Spycher, 2007). Properties correlated include density, viscosity, and specific enthalpy of the fluid phases as functions of temperature, pressure, and composition. Water properties are calculated from the International Formulation Committee (1967) steam table equations. Properties of pure CO_2 are obtained in tabular form from correlations developed by Altunin et al. (1975).

We neglect effects of dissolved water on the density and viscosity of the CO_2-rich phases. Brine density is calculated from the correlations of Haas (1976) and Andersen et al. (1992). The aqueous-phase density is calculated assuming additive volumes of brine and dissolved CO_2. Brine viscosity is obtained from a correlation by Phillips et al. (1981). Aqueous-phase viscosity does not depend on dissolved CO_2 concentration.

Brine specific enthalpy is calculated from the correlations developed by Lorenz et al. (2000). Aqueous-phase specific enthalpy is obtained by adding the enthalpies of the CO_2 and brine, and accounting for the enthalpy of dissolution of CO_2. The specific enthalpy of water dissolved in the CO_2-rich phases is identical to the enthalpy of saturated water vapor at the same temperature, and heat-of-dissolution effects are neglected. Specific enthalpy of the CO_2-rich phases is calculated by adding the specific enthalpies of the CO_2 and water components.

EXAMPLE SIMULATIONS AND DISCUSSION

We describe three simulations to provide model verification and an application example. The first two, a one-dimensional consolidation problem and a simulation exhibiting the Mandel-Cryer effect, are compared to analytical solutions. The last, pressure response and surface uplift occurring during a CO_2 sequestration project, shows a match of published results.

One-Dimensional Consolidation of a Double Porosity Medium

In the one-dimensional consolidation problem, a z-direction stress is applied to the top of a fluid-filled double porosity (fracture and matrix) porous rock column, instantaneously inducing a deformation and a pressure increase. Afterwards, fluid is allowed to drain out of the column top and the pressure dissipates. An analytical solution to this problem was presented by Wilson and Aifantis (1982). In their analysis, strain is uniaxial and z-direction stress is constant throughout the process.

We first simulate the load application to produce the pressure increase. We start from an unstrained state where pressure and mean stress are both equal, impose a greater mean stress at the system top to induce a pressure increase in the column, and let the system equilibrate. For

uniaxial deformation, mean stress, z-direction stress, and pressure are related by

$$\tau_m = \frac{1}{3}\frac{(1+\nu)}{(1-\nu)}(\tau_{zz} - \alpha P) + \alpha P \qquad (16)$$

and the constant z-direction stress is calculated from the imposed mean stress and the equilibrium pressure. Next, we simulate fluid drainage. The system is initially at the above equilibrated state. We set the pressure at the system top to the initial pressure. The mean stress at the system top is set as well, calculated from Equation 16 using the constant z-direction stress and the initial pressure. Fluid then drains out of the system top as the pressure returns to the initial value. We simulated this for a 400 m long column that contained 800 gridblocks (half fracture, half matrix). Initial pressure and mean stress were 5.0 MPa, and the imposed mean stress was 8.0 MPa. The resulting equilibrium pressure was 6.2 MPa, and the calculated z-direction stress was 9.8 MPa. We ran the drainage portion of the simulation for 4000 seconds with one-second time steps. Comparison of simulated fracture pressure with the analytical solution is shown in Figure 1, with excellent agreement.

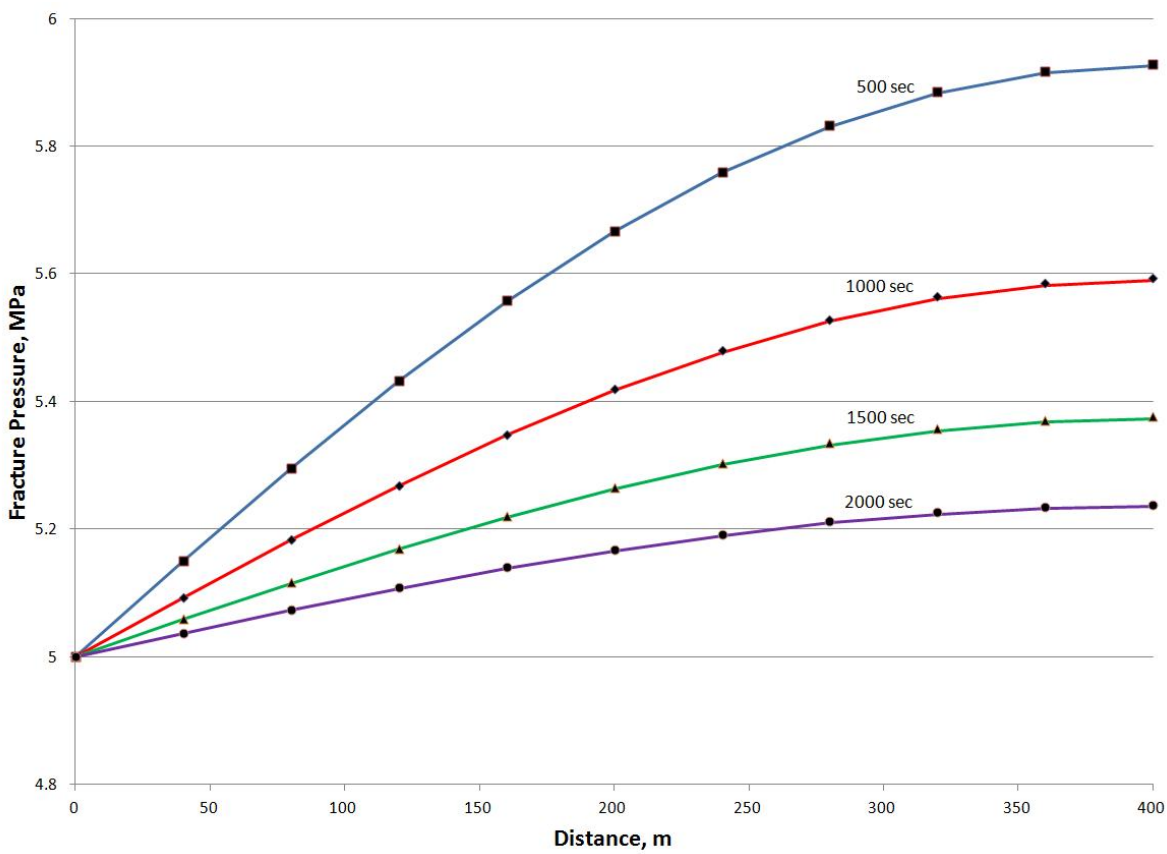

Figure 1. Comparison of analytical solution (solid lines) to simulation (points) for one-dimensional consolidation.

Mandel-Cryer Effect

Consider a poroelastic material that is allowed to drain laterally after a constant compressive force is applied to the top and bottom. Initially, a uniform pressure increase results from the undrained compression of the porous material. Because the pressure near the edges must decrease due to drainage, the material there becomes less stiff, and there is a load transfer to the center, resulting in a further increase in center pressure that reaches a maximum and soon declines due to fluid drainage. This pressure behavior is called the Mandel-Cryer effect (Mandel, 1953), and Abousleiman and Cheng (1996) present an analytical solution to the above process to which we compare our simulated results.

We first simulate the load application to produce the pressure increase. We start from an unstrained state where pressure and mean stress are both equal, impose a greater mean stress at the top and bottom to produce a pressure increase, and let the system equilibrate. Uniaxial stress is assumed in the analytical solution derivation, so mean stress and z-direction stress are related by

$$\tau_m = \frac{\tau_{zz}}{3} \tag{17}$$

Next, we simulate fluid drainage. The system is initially at the above equilibrated state, and we impose the initial pressure on the lateral boundaries to allow for drainage. We simulated this for a square with 1000 m sides that is subdivided into a 200×200 grid. The initial pressure and mean stress were 0.1 MPa, the applied z-direction stress was 3 MPa, and the equilibrium pressure was 2.18 MPa. The system drained for 50,000 seconds. We compare centerline pressure at the top with the analytical solution, shown in Figure 2. The simulated results exhibit the pressure maximum characteristic of the Mandel-Cryer effect and lie close to the analytical solution. The analytical solution and simulator formulation differ in that the analytical solution assumes that pressure varies only laterally; this could account for the difference in pressure peak heights.

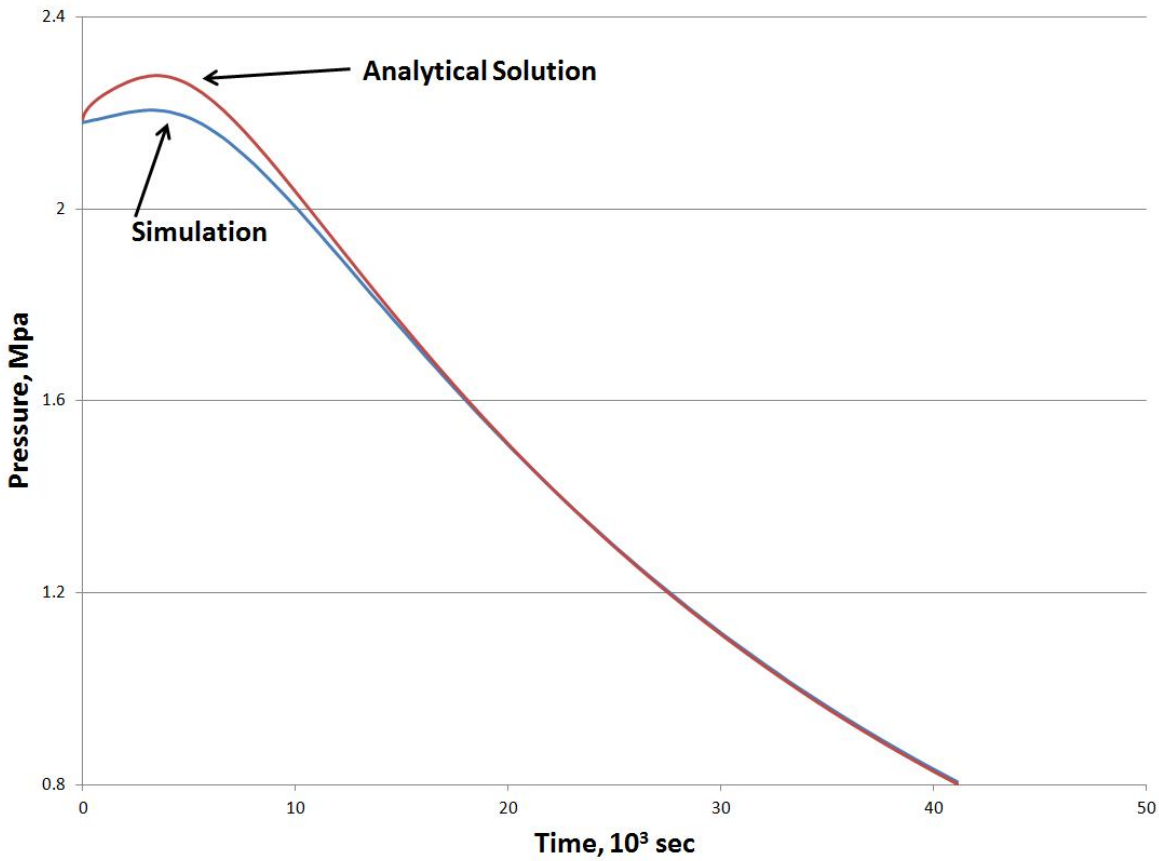

Figure 2. Comparison of analytical solution to simulation for Mandel-Cryer effect.

In Salah Project Simulation

The In Salah Gas Project, located in central Algeria, is a CO_2 storage project. Natural gas produced nearby is high in CO_2, and this CO_2 is injected back into the water leg of a depleting gas field for geological storage. Surface uplift from CO_2 injection has been measured by satellite-based inferrometry; Rutqvist et al. (2010) did a reservoir-geomechanical analysis of In Salah CO_2 injection and surface uplift using the TOUGH2-FLAC numerical simulator to determine if this uplift can be explained by pressure changes and deformation in the injection zone only. We reran their analysis on our code and used a cluster computer to demonstrate our parallel code's ability to simulate larger problems. Our cluster computer contains 16 nodes; each node has 24 GB of memory and two Intel® 5620 2.4GHZ 4-core processors.

The simulated domain was 10×10×4 km with one 1.5 km horizontal injection well at 1810 m depth and in the domain center. The domain consisted of four geological layers—Shallow Overburden, Caprock, Injection Zone, and Base—all with constant properties. CO_2 was injected for three years at 13.6 kg/sec. We simulated a 5×5×4 km quarter symmetry element of their system with a 1000×1000×60 grid (60 million grid-blocks). Figure 3 shows surface uplift, calculated by assuming strain isotropy, after three years of CO_2 injection, and Figure 4 is a comparison of surface uplift at the well's center versus depth to that of the reference.

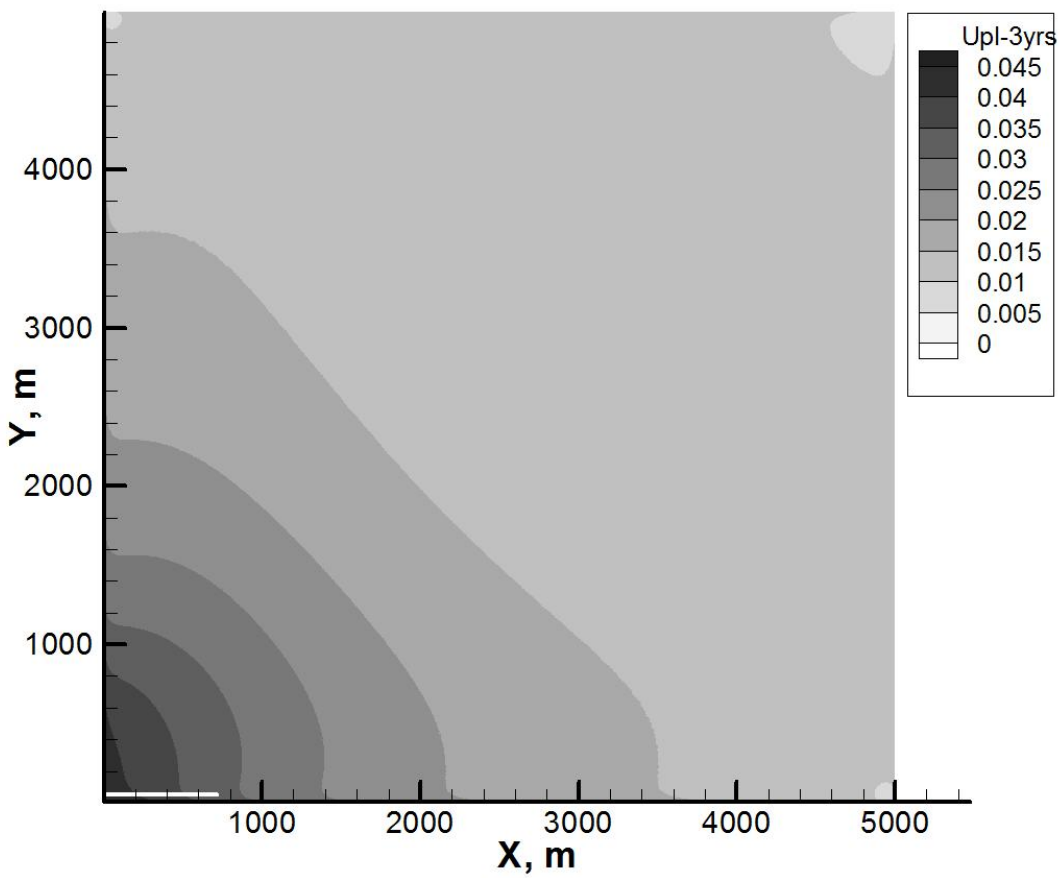

Figure 3. Surface uplift for quarter symmetry element; injection well shown by thick horizontal line at origin.

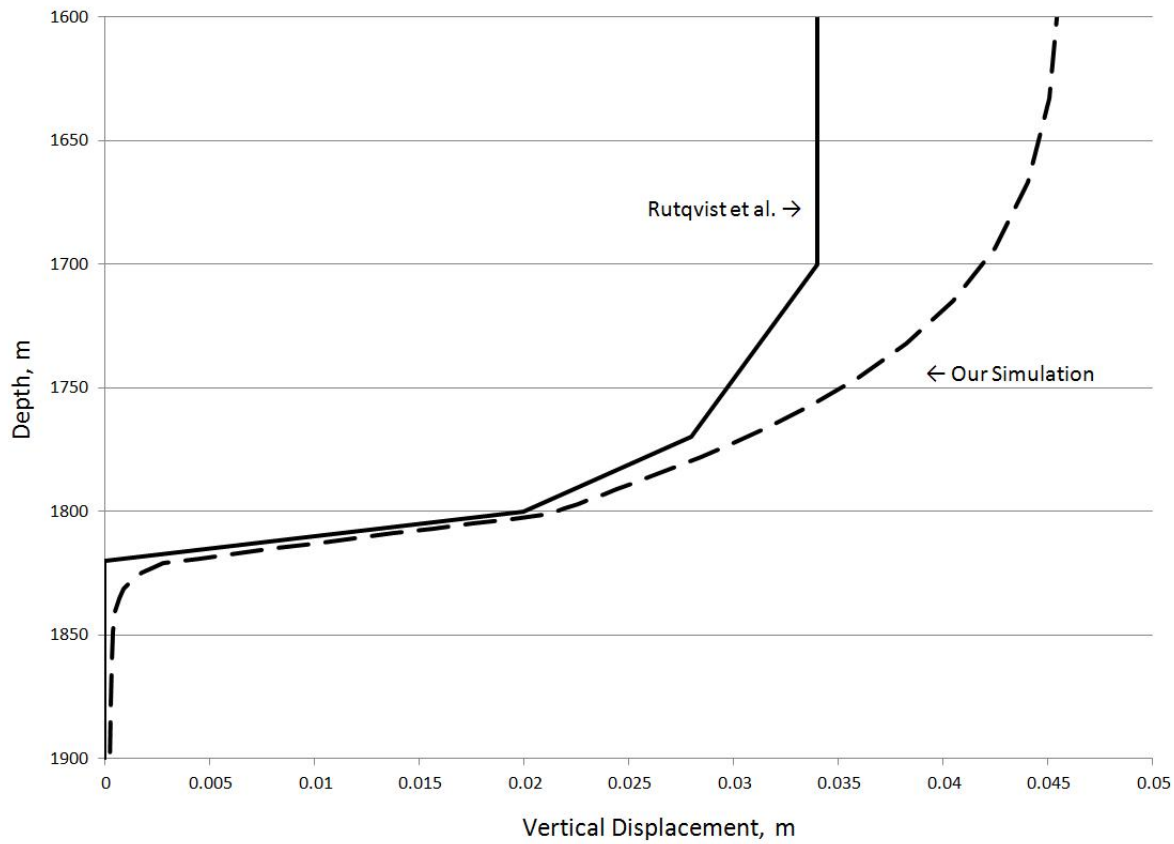

Figure 4. Comparison of surface uplift versus depth at well center.

CONCLUSIONS

We developed a massively parallel reservoir simulator for modeling THM processes in fractured and porous media saline aquifers. From the fundamental equations describing deformation of porous and fractured elastic media, we derived a conservation equation relating mean stress, pressure, and temperature, and incorporated it alongside the mass- and energy-conservation equations of TOUGH2-MP, the starting point for the simulator. In addition, rock properties, namely permeability and porosity, are functions of pressure and effective stress that are obtained from the literature.

We also developed an advanced fluid property module, ECO2M, which was designed for CO_2 sequestration in saline aquifers. It includes a description of the relevant properties of H_2O–NaCl–CO_2 mixtures that is highly accurate for the temperature, pressure, and salinity conditions of interest. Its fluid property correlations are identical to those of an earlier, less advanced fluid property module, but it allows liquid and gaseous CO_2-rich phases to be present, whereas the other does not distinguish between the two.

We verified the simulator formulation and numerical implementation, using analytical solutions and an example problem from the literature. For the former, we matched a one-dimensional consolidation problem and a two-dimensional simulation of the Mandel-Cryer effect. For the latter, we compared our results to those from two coupled computer codes, one that simulates fluid flow and heat transport, and another that simulates rock deformation. We obtained a good match of surface uplift after three years of CO_2 injection into the water leg of a depleting gas field. This agreement indicates that our formulation is able to capture THM effects modeled by a coupled simulation with a more detailed handling of rock mechanics.

ACKNOWLEDGMENT

This work was supported by the CMG Foundation and by the Assistant Secretary for Fossil Energy, Office of Coal and Power R&D through the National Energy Technology Laboratory under U.S. DOE Contract Number DE-FC26-09FE0000988.

REFERENCES

Abousleiman Y., A. H. D. Cheng, L. Cui, E. Detournay, J. C. Roegiers, Mandel's problem revisited, *Géotechnique*, 46**,** 187–95, 1996.

Altunin, V.V, *Thermophysical Properties of Carbon Dioxide,* Publishing House of Standards, 551 pp., Moscow, 1975 (in Russian).

Andersen, G., A. Probst, L. Murray, S. Butler, An Accurate PVT Model for Geothermal Fluids as Represented by H_2O-NaCl-CO_2 Mixtures, *Proc. 17th Workshop on Geothermal Res. Eng.,* 239 - 248, Stanford, CA, 1992.

Bai M., D. Elsworth, J.-C. Roegeirs, Modeling of naturally fractured reservoirs using deformation dependent flow mechanism, *Int. J. Rock Mech. Min. Sci. and Geomech. Abstr.,* 30(7), 1185-1191, 1993.

Davies J. P., D. K. Davies, Stress-dependent permeability characterization and modeling, *SPE 56813, pres. at ATCE*, Houston, TX, Oct. 1999.

Gutierrez M., R. W. Lewis, Petroleum reservoir simulation coupling fluid flow and geomechanics, *SPE Reservoir Evaluation & Engineering*, 164-72, June 2001.

Haas, J.L. Jr., Physical Properties of the Coexisting Phases and Thermochemical Properties of the H_2O Component in Boiling NaCl solutions, *USGS Bulletin 1421-A,* Washington, DC, 73 pp., 1976.

International Formulation Committee, *A Formulation of the Thermodynamic Properties of Ordinary Water Substance,* IFC Secretariat, Düsseldorf, Germany, 1967.

Mandel J., Consolidation des sols (etude mathematique), *Geotechnique,* 3287–99, 1953.

McTigue D. F., Thermoelastic response of fluid-saturated porous rock. *Journal of Geophysical Research*, 91(9), 9533-42, 1986.

Ostensen R. W., The effect of stress-dependent permeability on gas production and well testing, *SPE Form Eval*, 227–35, June 1986.

Phillips, S.L., A. Igbene, J.A. Fair, H. Ozbek and M. Tavana, A Technical Databook for Geothermal Energy Utilization, *Lawrence Berkeley National Laboratory Report LBL-12810*, Berkeley, CA, 46 pp., 1981.

Pruess K, *ECO2M: A TOUGH2 Fluid Property Module for Mixtures of Water, NaCl, and CO_2, Including Super- and Sub-Critical Conditions, and Phase Change Between Liquid and Gaseous CO_2,* Lawrence Berkeley National Laboratory Report LBL-4590E, 2011.

Pruess K. and N. Spycher, ECO2N – A Fluid Property Module for the TOUGH2 Code for Studies of CO2 Storage in Saline Aquifers, *Energy Conversion and Management,* 48(6), 1761–1767, 2007.

Rutqvist J., C.-F. Tsang, A study of caprock hydromechanical changes associated with CO_2-injection into a brine formation, *Environmental Geology* 42, 296–305, 2002.

Rutqvist J., D. W. Vasco, L. Myer, Coupled reservoir-geomechanical analysis of CO_2 injection and ground deformations at In Salah Algeria, *Int. J. of Greenhouse Gas Control*, 4, 225–30, 2010.

Spycher, N., K. Pruess, CO_2-H_2O Mixtures in the Geological Sequestration of CO_2. II. Partitioning in Chloride Brines at 12–100 °C and up to 600 bar, *Geochim. Cosmochim. Acta,* 69(13), 3309–3320, 2005.

Verma A., K. Pruess, Thermohydrological conditions and silica redistribution near high-level nuclear wastes emplaced in saturated geological formations, *J Geophys Res*, 93, 1159-73, 1988.

Wilson R. K., E. C. Aifantis, On the theory of consolidation with double porosity, *Int. J. Eng. Sci,*. 20(9), 1009-35, 1982.

Zhang K., Y.-S. Wu, K. Pruess, *User's guide for TOUGH2-MP - a massively parallel version of the TOUGH2 code,* Lawrence Berkeley National Laboratory Report LBNL-315E, 2008.

Zimmerman R. W., W. H. Somerton, M. S. King, Compressibility of porous rocks, *J Geophys Res,* 91(12), 765–77, 1986.